Hyperspectral Imaging of Wounds Reveals Augmented Tissue Oxygenation Following Cold Physical Plasma Treatment *in Vivo*

Anke Schmidt, Felix Nießner, Thomas von Woedtke, and Sander Bekeschus, *Member, IEEE*

***Abstract*—Efficient vascularization of skin tissue supports wound healing in response to injury. This includes elevated blood circulation, tissue oxygenation, and perfusion. Cold physical plasma promotes wound healing in animal models and humans. Physical plasmas are multicomponent systems that generate several physicochemical effectors, such as ions, electrons, reactive oxygen and nitrogen species, and UV radiation. However, the consequences of plasma treatment on wound oxygenation and perfusion, vital processes to promote tissue regeneration, are largely unexplored. We used a novel hyperspectral imaging (HSI) system and a murine dermal full-thickness wound model in combination with kINPen argon plasma jet treatment to address this question. Plasma treatment promoted tissue oxygenation in superficial as well as deep (6 mm) layers of wound tissue. In addition to perfusion changes, we found a wound healing stage-dependent shift of tissue hemoglobin and tissue water index during reactive species-driven wound healing. Contactless, fast monitoring of medical parameters in real-time using HSI revealed a plasma-supporting effect in wound healing together with precise information about biological surface-specific features.**

***Index Terms*—Full-thickness skin wounds, mouse model, plasma medicine, reactive oxygen and nitrogen species, skin microcirculation.**

I. Introduction

THE TREATMENT of wound healing associated pathologies (e.g., venous leg, diabetic foot, or pressure ulceration) remains a global medical challenge to wound care professionals. Healthcare resources and costs associated with the management of patients with chronic wounds are enormous and are rising continuously [1], [2]. Wound healing is disrupted if one of the phases hemostasis, inflammation, reepithelialization, and remodeling do not progress to the next phase, with various pathophysiological consequences [3].

Manuscript received May 25, 2020; revised June 29, 2020; accepted July 9, 2020. Date of publication July 17, 2020; date of current version May 3, 2021. This work was supported in part by the Ministry of Education, Science, and Culture of the State of Mecklenburg–Western Pomerania, Germany; in part by the European Union, European Social Fund under Grant AU 11 038, Grant ESF/IV-BM-B35-0010/13, and Grant AU 15 001; and in part by the German Federal Ministry of Education and Research under Grant 03Z22DN11 and Grant 03Z22Di1. *(Corresponding author: Anke Schmidt.)*

Anke Schmidt, Felix Nießner, and Sander Bekeschus are with the ZIK plasmatis, Leibniz Institute for Plasma Science and Technology (INP), 17489 Greifswald, Germany (e-mail: anke.schmidt@inp-greifswald.de).

Thomas von Woedtke is with the ZIK plasmatis, Leibniz Institute for Plasma Science and Technology (INP), 17489 Greifswald, Germany, and also with the Institute for Hygiene and Environmental Medicine, Greifswald University Medical Center, 17489 Greifswald, Germany.

Digital Object Identifier 10.1109/TRPMS.2020.3009913

A key local factor for proper wound outcome is adequate perfusion of appropriate regions with oxygenated blood to avoid hypoxic conditions being one characteristic of nonhealing wounds [4]. Especially tissue oxygenation and hemoglobin levels are critical physiological factors affecting healing [3]. In living cells, oxygen induces several imperative physiological processes, such as migration and differentiation [5], remodeling of actin and collagen architecture [6], prevention of wound infections via superoxide production in leukocytes [7], and promotion of angiogenesis [3]. Macrophages play a beneficial role in directing angiogenesis by releasing pro-angiogenic factors [8], [9]. If wound oxygenation is not impaired, subsequent healing processes are interrupted, including proliferative, migratory, apoptotic, and chemotactic processes, which are closely associated with cellular cytokine and growth factor secretion and downstream signaling [10].

Reactive oxygen and nitrogen species (here summarized as ROS)-driven signaling pathways contribute to physiological wound healing. ROS act as cellular messengers to stimulate key wound healing processes [11]–[13]. Cold physical plasma medical systems such as the kINPen generate ROS [14] that were linked to accelerated wound healing in humans [15]–[23]. A range of coordinated processes in epithelial wound coverage, cell spreading, migration via modulation of integrin adhesion, collagen deposition, matrix degradation, and neovascularization has been shown in animal models following plasma treatment [24]–[27]. Monitoring wound oxygenation and perfusion with optical-based techniques play an essential part in wound management in clinics [28]. Given the importance of oxygen supply in the blood, the role of plasma in microcirculatory features, such as tissue oxygenation and perfusion status remains largely elusive.

Hyperspectral imaging (HSI) is an emerging imaging modality for medical applications [29] and seems to be suitable for routine diagnostics and monitoring of skin tissue injuries in acute or chronic wounds [30]–[33], and other skin diseases [34]. It allows the identification of hyperspectral characteristics of biological surfaces, depending on its biochemical and structural features in terms of spectral ranges and their dynamics over time [35]. HSI combines spectroscopy, imaging data acquisition, and digital image processing to allow for a noninvasive, contactless assessment of tissue parameters. Medical HSI camera systems record a spectral range

between 500 and 1000 nm with a dispersion of approximately 100 wavelengths [10]. This provides 3-D data on tissue oxygenation in the microcirculation in superficial layers and the perfusion of deeper tissue parts. Due to the higher penetration depth of far and infrared light in tissues, the distribution of hemoglobin [36] and the water content of tissue [29] can be determined in real time and with spatial solution [37]–[39].

We here aimed at investigating the tissue oxygenation and perfusion parameters in wounds following plasma treatment and using noninvasive HSI in an immunocompetent SKH1 mouse model. Moreover, the quantification of microcirculatory parameters allowed us to find a specific fingerprint of physiological wound healing after plasma treatment.

II. Experimental Design

A. Animal Model and Plasma Treatment

Our study was conducted in accordance with the local ethics committee and the guidelines for the care and use of laboratory animals (Az.: 7221.3-1-044/16). SKH1 mice were housed under standard conditions in an animal facility (Institute of Pharmacology of University of Greifswald, Germany). The standardized generation of full-thickness skin wounds in a mouse model was done as previously described [24], [27]. Briefly, ear wounds were made by the removal of epidermal and dermal skin layers after anesthesia by ketamine and xylazine. The local application of plasma (10 s) was performed every third day over 14 consecutive days using the kINPen MED (neoplas tools, Greifswald, Germany). The kINPen ionized argon gas (purity 99.9999%; Air Liquide, Krefeld, Germany) at 1 MHz at five standard liters per second of argon. The plasma treatment was standardized using the tip of the plasma effluent at a constant distance of 8 mm using an autoclavable spacer. Untreated mice served as controls.

B. Hyperspectral Imaging

The HSI camera system *TIVITA Tissue* (Diaspective Vision, Pepelow, Germany) was utilized to analyze the tissue characteristics in real time across a range of wavelengths (500–1000 nm) without the use of contrast agents. The parameters that can be retrieved by HSI spectra via software algorithms include tissue oxygenation (StO_2) in superficial layers, the perfusion into deeper skin regions of 4–6 mm (near-infrared index, NIR), the tissue hemoglobin index (THI) with monitoring of the percental volume of hemoglobin of surface perfusion, and the tissue water index (TWI). The working distance from the camera to the mouse ear was 50 cm, and each hyperspectral image was acquired under standardized conditions (darkroom and the same exposure times). The measurements started with a baseline analysis of healthy skin to assess the tissue parameters and background levels. After wounding, HSI parameters were recorded 10 min after plasma treatment and compared to that of untreated controls ($n \geq 4$). Controls were set to 1. The camera-specific software *TIVITA Suite* calculates parameters in well-defined circular areas, including wound regions (pink), blood vessels (purple), and background of ear skin (gray). All measurements were recorded every third day up to the endpoint (d15).

TABLE I
HSI and Four Medical Parameters That Can Be Retrieved From Visible to Near-Infrared Range

Parameter	Spectral range (nm)	Feature characterization	Evaluated spectral range (nm)
StO_2	530 – 600 730 – 800	Relative tissue oxygenation in the superficial layer (1 mm)	550 – 575 750 - 775
THI	650 - 730 820 - 930	Relative tissue oxygenation in deeper layers (4 - 6 mm)	650 – 730 820 – 870/ 900 - 930
NIR	530 – 590 730 - 820	Distribution of hemoglobin in skin tissue	570- 590 790 - 810
TWI	879 – 900 950 - 975	Water content and distribution in skin tissue	870 – 900 950 - 975

StO_2 = oxygenation, weber, THI = tissue hemoglobin index, NIR = near infrared index, TWI = tissue water index.

C. Statistical Analysis

Data are presented as mean +S.E. statistical analysis of the StO_2, NIR, THI, and TWI indexes was done using one-way analysis of variance (ANOVA) with p-values indicated by $^{*}p < 0.05$,$^{**}p < 0.01$, and $^{***}p < 0.001$. The graphing and analysis was performed using GraphPad prism 7.04 (San Diego, CA, USA).

III. Results

A. Optical Diagnostic of Cutaneous Tissue Using HSI

The interactions of light with skin tissue is determined by intrinsic optical features of the skin surface [40]. Mammalian skin is composed of mainly two layers, including the epidermis with stratum corneum (SC), and the dermis along with blood vessels. Light of different wavelengths penetrate the tissue up to 6-mm deep, but most of the light interacts with the skin, resulting in changes of absorption, reflection, remission, and transmission to its internal layers. Visible light (VIS) is highly absorbed, resulting in lower penetration depth, whereas near-infrared (NIR) light is much less absorbed, resulting in larger penetration depths. The subcutaneous tissue (subcutis) lies below the dermis and does not affect the light very much [Fig. 1(a)].

Next, the absorption spectrum of the light scattered back was recorded using an HSI camera system. Different parts of the spectrum in the range between 500 and 1000 nm were used for the calculation of four different medical parameters [Fig. 1(b)].

The tissue oxygenation StO_2 describes the relative oxygenation in superficial tissue layers in 1-mm penetration depth. It was measured in two spectral ranges between 530–600 nm and 730–800 nm. The tissue hemoglobin index for distribution of hemoglobin (THI) was determined in the range of 530–590 nm and 730–820 nm. The near-infrared perfusion index in deeper tissue layers (NIR) was calculated from the intensities in the ranges between 650–730 nm and 820–930 nm. The tissue water index for water distribution (TWI) was measured in the range between 870–900 nm and 950–975 nm (Table I).

B. HSI of Uncompromised and Wounded Murine Skin Tissue

The first assessment of skin tissue parameters was done using HSI of uncompromised, healthy mouse ear skin (RGB

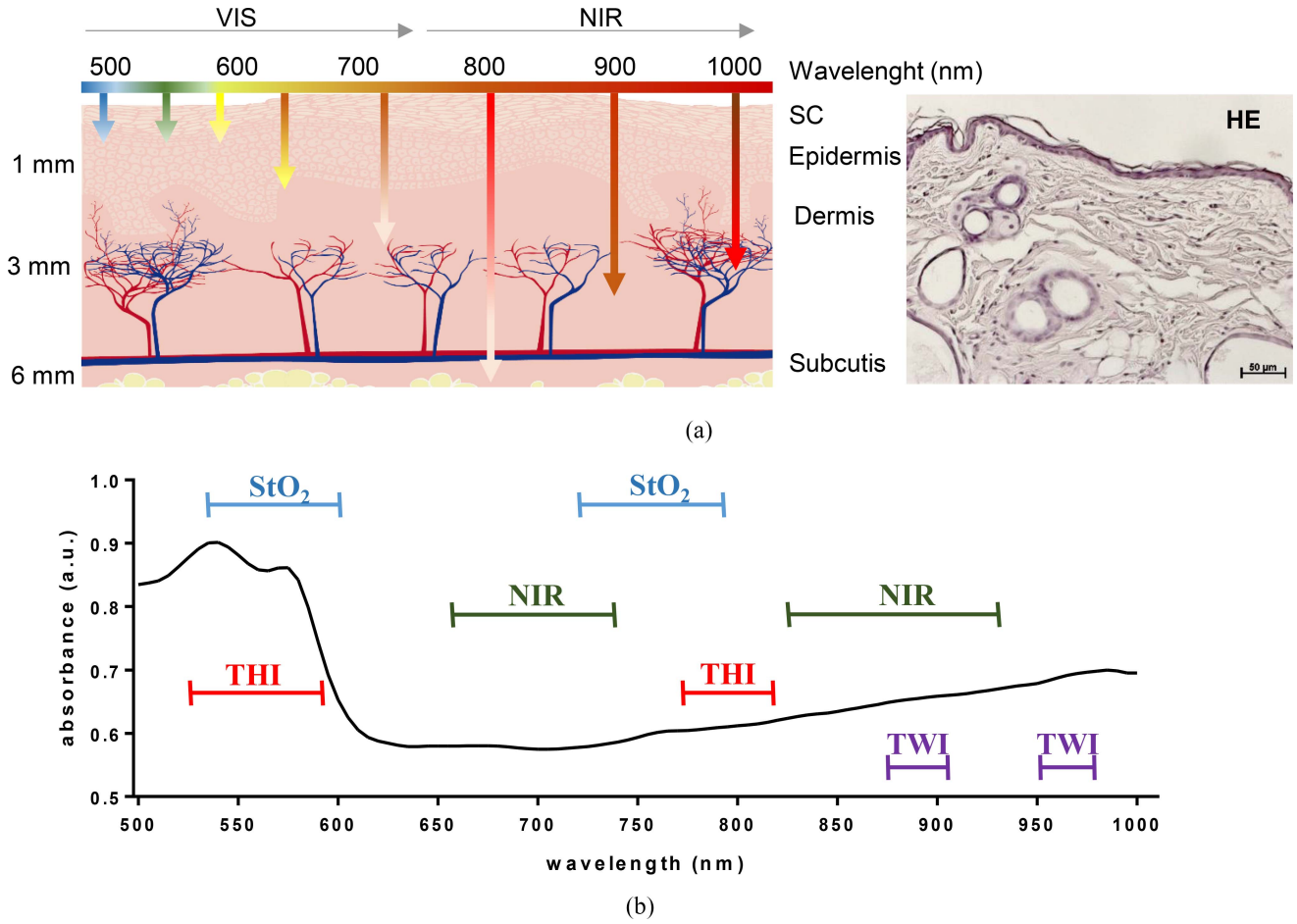

Fig. 1. Light absorption in skin tissue and spectra of the parameters measured. (a) Schematic illustration (left) and hematoxylin and eosin staining (HE, right) of the skin showing the epidermis including SC and the dermis including blood vessels. Subcutis is not part of the skin. Scale bar 50 μm. Light of different wavelengths penetrate the tissue in layers as deep as 6 mm and interact with the biological surface resulting in changes of absorption, reflection, remission, and transmission. Tissue readily absorbs light in the visible (VIS) range, resulting in only low penetration depth. In contrast, light in the near infrared (NIR) range is much less absorbed, resulting in higher penetration depths. (b) Representative spectral analysis of healthy skin. High-resolution HSI in the range of 500–1000 nm allows for the calculation of a total of four parameters from the spectral information. StO2, tissue oxygenation for relative oxygenation in superficial tissue layers; NIR, near-infrared perfusion index in deeper tissue layers; THI, tissue hemoglobin index for distribution of hemoglobin; and TWI, tissue water index for water content.

image). A typical skin tissue absorption spectrum was recorded at wavelengths ranging from visible to near-infrared spectrum in three regions: 1) the wound (here identical with background signal, pink); 2) blood vessels (purple); and 3) skin background (gray) [Fig. 2(a)]. For the analysis of tissue parameters in skin injury, a dermal full-thickness wound was created (arrow in the RGB image), and absorption data from 500 to 1000 nm were acquired in real time using the HSI camera system [Fig. 2(b)]. Additionally, physicochemical information and microcirculatory parameters of skin tissue were recorded and shown as pseudo-color images of health [Fig. 2(c)], and wounded ear skin [Fig. 2(d)]. HSI measurements showed higher surface oxygen saturation and tissue hemoglobin distribution in the wound zone in comparison to healthy skin (arrows).

C. HSI Reveals Tissue Parameter Modulation in Wound Following Plasma Treatment

The plasma-induced beneficial effects in neovascularization have been reported in previous studies [27], [41]–[43] suggesting that the hemodynamically relevant parameters provided by HSI allow deeper insights into microcirculation, their parameters, and kinetics. After wounding (d0), HSI measurements were performed every third day after plasma treatment (red mice) and compared to those of untreated controls [white mice, Fig. 3(a)]. The wound healing process was visualized in RGB images from day 0 to the endpoint of measurements on d15. Additionally, we monitored the plasma-induced microcirculatory changes, such as the grade of tissue oxygenation, perfusion, hemoglobin, and water content throughout the healing process using pseudo-colored images generated by the HSI software. The wound regions are highlighted when noticeable changes were visible [arrows, Fig. 3(b)–(e)]. Changes in the oxygenation in superficial layers [StO_2, Fig. 3(b)] and hemoglobin perfusion [THI, Fig. 3(d)] in wound regions after treatment were apparent, particularly on d0, d3, and d12.

The HSI software allows quantification of the integrated spatial distribution of oxygenation and the other microcirculation-dependent values. The spectral signals for each microcirculatory parameter at the corresponding wavelengths were quantified after plasma treatment (red boxes),

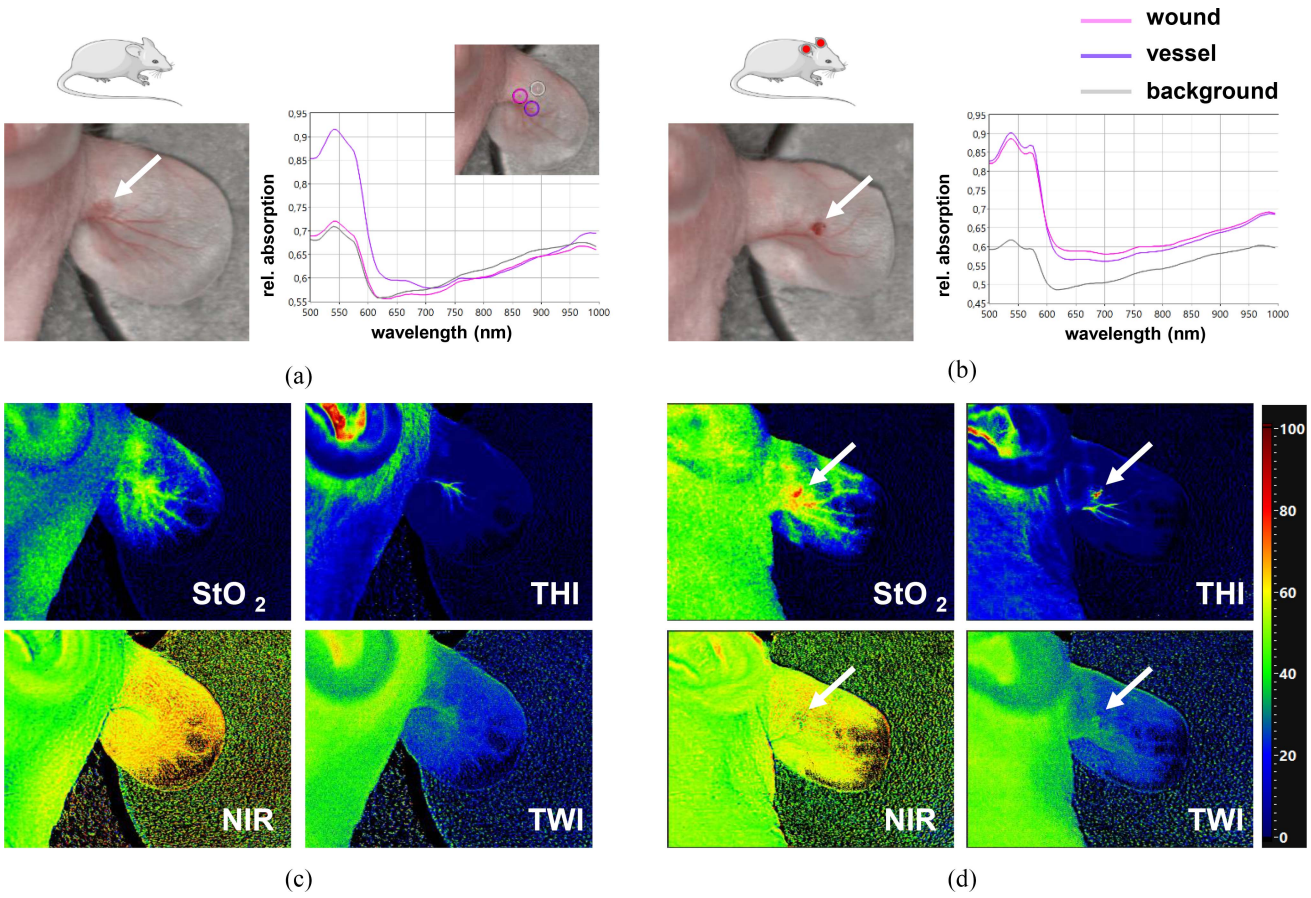

Fig. 2. HSI of tissue oxygenation and perfusion in healthy and injured skin. HSI was used for the noninvasive acquisition of tissue parameters in a dermal full-thickness ear wound model in SKH1 mice. Acquisition of RGB color images and typical spectra of different regions for the determination of microcirculatory parameters in healthy (a) and injured skin (b). Selections of three regions, including background (gray), wound (pink), and blood vessels (purple), were visualized on the ear tissue surface via HSI [small image in (a)]. From the spectral data, several features were filtered, including tissue oxygenation (StO_2), near-infrared perfusion of tissue (NIR), tissue hemoglobin index (THI), and tissue water index (TWI) in both healthy (c) and injured (the wound region is marked with an arrow) skin (d).

and compared to that of untreated controls (white boxes) after normalization to background signals. The results for tissue oxygenation (StO_2) of the blood microcirculatory system in the visible spectral regions (up to 600 nm) reflect the oxygenation up to 1-mm deep into the tissue, demonstrating a significantly higher absorbance on d0, d3, d9, and d12 in plasma-treated animal wounds [Fig. 3(b)]. Comparable results were obtained for cutaneous oxygen saturation and perfusion in deeper layers (near-infrared spectral range). NIR indices within the wound region were significantly increased on days 0, 3, 6, and 12 [Fig. 3(c)]. Oxygenation in superficial and deeper layers remained unchanged at the endpoint of measurements (d15). Analysis of hemoglobin concentration (THI) revealed a significant increase at the beginning (d0) as well as on days 3 and 12 when compared to controls [Fig. 3(d)]. Furthermore, we obtained a significant decrease of the tissue water index (TWI) on day 9 in the plasma treatment group. However, water content fluctuated during the following six days. While the absorption was initially higher in plasma-treated animals and in comparison to control on d12, the TWI eventually dropped significantly below the levels of untreated controls on day 15, which is indicative of an absence of tissue edema and accelerated wound healing [Fig. 3(e)]. Moreover, we found no abnormalities or disturbing behavior in animals of the plasma-treated groups.

IV. Discussion

An important issue in nonhealing wounds is the impaired angiogenic response and vascularization due to the absence of adequate perfusion and tissue oxygenation [44]. Therefore, understanding the tissue oxygenation and *de-novo* formation of new blood vessels during wound healing helps to attain better therapeutic strategies and facilitates accelerated healing of problematic wounds in patients. One critical factor that is essential in making the wound environment receptive to therapies is the correction of wound hypoxia [13].

Cold physical plasma is antimicrobial [45] and promotes wound healing potential also wound-relevant immune processes [23], [46]. Recent reports emphasize the importance of ROS regulating inflammation and subsequently tissue vascularization [11]–[13], [47]–[50]. Vascular endothelial growth factor, angiopoietin, fibroblast growth factor, and transforming growth factor beta are among the most potent angiogenic cytokines in wound angiogenesis [51], which were also identified in several plasma-treated skin cells and

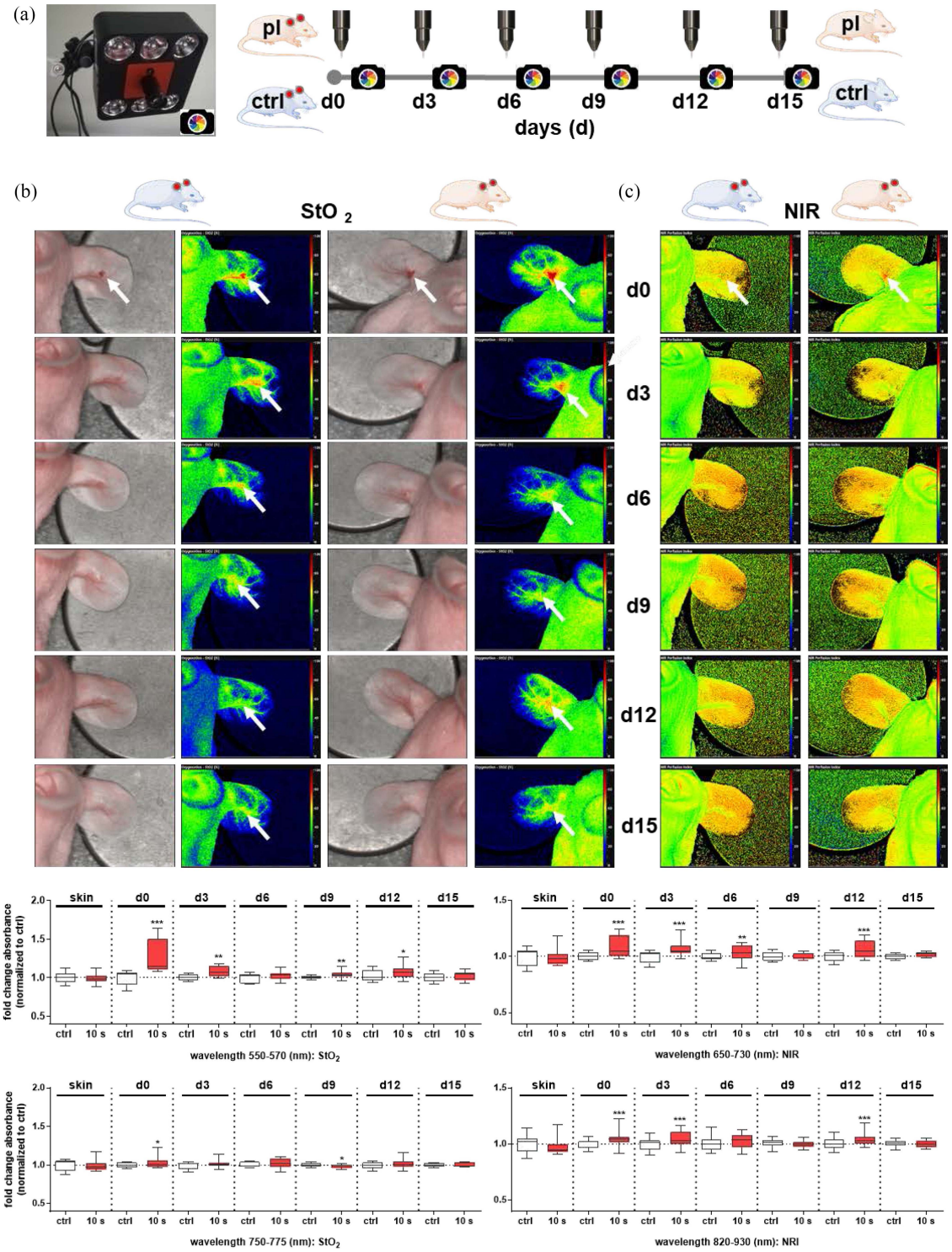

Fig. 3. HSI analysis of injured tissue after plasma treatment. (a) After plasma treatment (red mice), the wound healing process was monitored every third day (endpoint d15) using HSI (left picture) and compared to untreated controls (gray mice). (b)–(e) Representative colored RGB images with corresponding pseudo-false images of microcirculatory features are given for d0, d3, d6, d9, d12, and d15. Various features from the spectral data were filtered out, including tissue oxygenation [StO_2, (b)], near-infrared index [NIR, (c)], tissue hemoglobin index [THI, (d)], and tissue water index [TWI, (e)]. The spectral intensities of each microcirculatory parameter were quantified over time, and the fold changes of absorbance of the plasma-treated group (red boxes) were normalized to that of untreated controls (white boxes) and set to 1. For StO_2, spectral ranges between 550–570 nm and 750–775 nm were used (b). NIR was analyzed between 650 and 730 nm and two other spectral ranges between 820–870 nm and 900–930 nm, which were summarized into one diagram from 820 to 930 nm (c). THI was evaluated between 570–590 nm and 790–810 nm (d). TWI was recorded between 870–900 nm and 950–975 nm (e). Statistical analysis was performed using one-way ANOVA between plasma-treated and untreated mice with $^{*}p < 0.05$,$^{**}p < 0.01$, and $^{***}p < 0.001$ ($n \geq 4$ wounds/group).

mice [27], [52], [53]. Despite advances in plasma-driven healing of chronic wounds in humans [23], the plasma effects on tissue oxygenation and perfusion status that are vital in determining wound healing outcomes are sparse. Objective imaging and metrics of healing are capable of providing important information that is independent of subjective visual

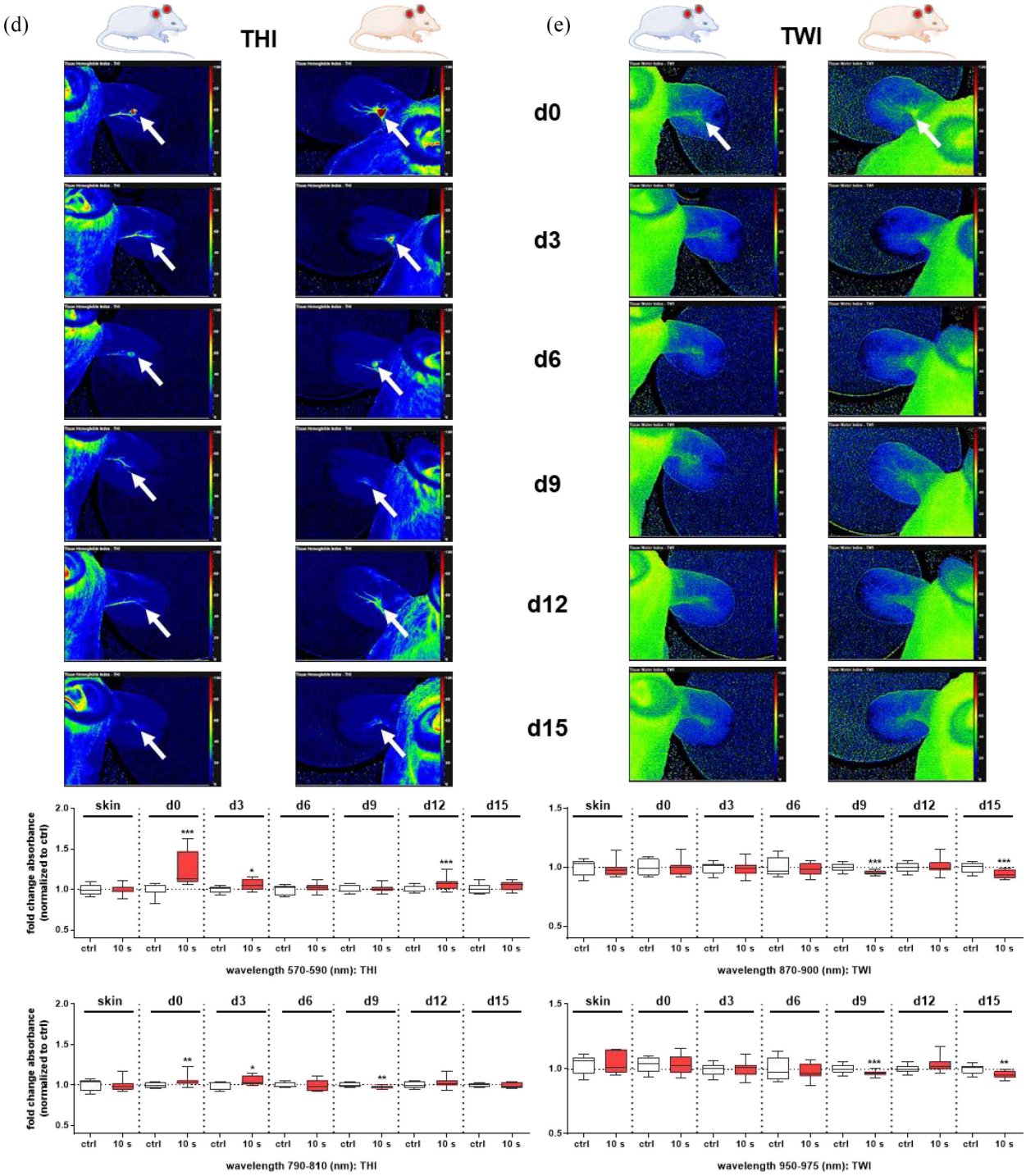

Fig. 3. To be Continued.

inspection of wounds as it still is standard in the clinics. Moreover, biological surfaces such as skin tissue exhibit useful optical properties in the visible and near-infrared electromagnetic spectrum [10].

A compact HSI camera system was used, enabling the investigation of tissue oxygenation (StO_2), perfusion, hemoglobin, and water distribution during wound healing and plasma treatment in a murine wound model. The analysis of microcirculatory features revealed remarkable differences between plasma-treated and untreated wounds. Next to the acceleration of wound healing [24], [27], [54], we obtained an improvement of StO_2 and NRI in the early phases of wound closure, implicating plasma-triggered oxygenation and perfusion. Moreover, dynamic changes over time were observed for optical THI signals. A clear increase of the hemoglobin levels was shown in response to plasma, particularly on early time points. This finding validates previous results from intravital microscopy, demonstrating accelerated neovascularization in association with a significantly higher blood vessel outgrowth in plasma-treated mice [27]. In patients, complex blood perfusion was determined in a chronic wound caused by peripheral arterial occlusive disease (PAOD), showing stimulating

plasma effects with elevated oxygenation and hemoglobin parameters [33]. In mice, we found a switch from an initially high to later low water content, indicating a decrease of edema after plasma treatment in injured skin tissue that enabled increased diffusion of oxygen to support cellular metabolism and growth. Edema occurs when an excessive volume of fluid accumulates either in cells or within the collagen matrix of tissue [55].

While most of the optical techniques for measuring of oxygenation parameters such as laser Doppler fluxometry with transcutaneous oxygen monitoring [56], [57], as well as tissue oximeters [58], penetrate up to 1–2 mm from wound surface, HSI has the archives deeper layers up to 6 mm similar to NIR spectroscopy [10]. The HSI technology was translated into medicine in several medical applications in recent years. It offers excellent potential for noninvasive disease diagnosis and surgical guidance [29]. The measurement of perfusion parameters was successfully monitored using HSI in healthy skin [37], [59], in wounds following the application of a microcapillary dressing [38], in a rat model of surgically induced ischemia after microvascular anastomosis [31], and in skin diseases like human melanoma [34]. Generally, HSI has apparent advantages in determining microcirculatory parameters with imaging measurements in real time and spatial resolution without adverse effects on, e.g., local cutaneous microcirculation [38]. HSI also serves as an alternative for invasive tissue sampling and downstream analysis with the benefit of the reflectance spectrum being related to metabolic activity and perfusion. Such a correlation between cellular status and spectral signatures was demonstrated in a 3-D wound model *in vitro* [35]. Finally, spectral analysis is being done using nonionizing light, making this approach safe for use in humans.

V. Conclusion

Cold plasma treatment increases oxygen delivery through increase perfusion, ultimately supporting tissue angiogenesis and wound healing features. Using HSI, we were able to demonstrate significantly different absorption spectra between plasma-treated and untreated wounds in the early and late phases of wound healing. The noninvasive HSI revealed a plasma-triggered increase of oxygen saturation and perfusion as well as hemoglobin concentration with decreased water content in injured tissue. Consequently, the determination of physiological tissue parameters by HSI evidenced cold physical plasma as a promising tool for chronic wound healing. HSI may help to image wound healing in clinical diagnostics in humans quickly and straightforwardly.

Acknowledgment

The authors thank Bernhard Rauch and Markus Grube (both Institute of Pharmacology, University of Greifswald) for support with animal housing.

References

[1] S. Morbach *et al.*, "Long-term prognosis of diabetic foot patients and their limbs: Amputation and death over the course of a decade," *Diabetes Care*, vol. 35, no. 10 pp. 2021–2027, Oct. 2012, doi: 10.2337/dc12-0200.

[2] N. R. Barshes *et al.*, "The system of care for the diabetic foot: Objectives, outcomes, and opportunities," *J. Diabet. Foot Ankle*, vol. 4, no. 1, Oct. 2013, Art. no. 21847, doi: 10.3402/dfa.v4i0.21847.

[3] S. Guo and L. A. Dipietro, "Factors affecting wound healing," *J. Dental Res.*, vol. 89, no. 3, pp. 219–29, Mar. 2010, doi: 10.1177/0022034509359125.

[4] A. A. Tandara and T. A. Mustoe, "Oxygen in wound healing—More than a nutrient," *World J. Surg.*, vol. 28, no. 3, pp. 294–300, Mar. 2004, doi: 10.1007/s00268-003-7400-2.

[5] P. G. Rodriguez, F. N. Felix, D. T. Woodley, and E. K. Shim, "The role of oxygen in wound healing: A review of the literature," *Dermatol. Surg.*, vol. 34, no. 9, pp. 1159–69, Sep. 2008, doi: 10.1111/j.1524-4725.2008.34254.x.

[6] T. R. Cox and J. T. Erler, "Remodeling and homeostasis of the extracellular matrix: Implications for fibrotic diseases and cancer," *Disease Models Mech.*, vol. 4, no. 2, pp. 165–78, Mar. 2011, doi: 10.1242/dmm.004077.

[7] A. Bishop, "Role of oxygen in wound healing," *J. Wound Care*, vol. 17, no. 9, pp. 399–402, Sep. 2008, doi: 10.12968/jowc.2008.17.9.30937.

[8] T. J. Koh and L. A. DiPietro, "Inflammation and wound healing: The role of the macrophage," *Expert Rev. Mol. Med.*, vol. 13, p. e23, Jul. 2011, doi: 10.1017/S1462399411001943.

[9] B. M. Delavary, W. M. van der Veer, M. van Egmond, F. B. Niessen, and R. H. Beelen, "Macrophages in skin injury and repair," *Immunobiology*, vol. 216, no. 7, pp. 753–62, Jul. 2011, doi: 10.1016/j.imbio.2011.01.001.

[10] M. G. Sowa, W. C. Kuo, A. C. Ko, and D. G. Armstrong, "Review of near-infrared methods for wound assessment," *J. Biomed. Opt.*, vol. 21, no. 9, Sep. 2016, Art. no. 091304, doi: 10.1117/1.JBO.21.9.091304.

[11] C. K. Sen, "The general case for redox control of wound repair," *Wound Repair Regeneration*, vol. 11, no. 6, pp. 431–8, Nov./Dec. 2003. [Online]. Available: https://www.ncbi.nlm.nih.gov/pubmed/14617282.

[12] C. K. Sen, "Wound healing essentials: Let there be oxygen," *Wound Repair Regeneration*, vol. 17, no. 1, pp. 1–18, Jan./Feb. 2009, doi: 10.1111/j.1524-475X.2008.00436.x.

[13] C. K. Sen and S. Roy, "Redox signals in wound healing," *Biochimica et Biophysica Acta*, vol. 1780, no. 11, pp. 1348–61, Nov. 2008, doi: 10.1016/j.bbagen.2008.01.006.

[14] S. Reuter, T. von Woedtke, and K. D. Weltmann, "The kINPen—A review on physics and chemistry of the atmospheric pressure plasma jet and its applications," *J. Phys. D Appl. Phys.*, vol. 51, no. 23, Jun. 2018, Art. no. 233001, doi: 10.1088/1361-6463/aab3ad.

[15] G. Isbary *et al.*, "Successful and safe use of 2 min cold atmospheric argon plasma in chronic wounds: Results of a randomized controlled trial," *Brit. J. Dermatol.*, vol. 167, no. 2, pp. 404–10, Aug. 2012, doi: 10.1111/j.1365-2133.2012.10923.x.

[16] G. Isbary *et al.*, "A first prospective randomized controlled trial to decrease bacterial load using cold atmospheric argon plasma on chronic wounds in patients," *Brit. J. Dermatol.*, vol. 163, no. 1, pp. 78–82, Jul. 2010, doi: 10.1111/j.1365-2133.2010.09744.x.

[17] G. Isbary, T. Shimizu, J. L. Zimmermann, H. M. Thomas, G. E. Morfill, and W. Stolz, "Cold atmospheric plasma for local infection control and subsequent pain reduction in a patient with chronic post-operative ear infection," *New Microbes New Infections*, vol. 1, no. 3, pp. 41–3, Dec. 2013, doi: 10.1002/2052-2975.19.

[18] G. Isbary *et al.*, "Cold atmospheric argon plasma treatment may accelerate wound healing in chronic wounds: Results of an open retrospective randomized controlled study *in vivo*," *Clin. Plasma Med.*, vol. 1, no. 2, pp. 25–30, 2013, doi: 10.1016/j.cpme.2013.06.001.

[19] H. R. Metelmann, C. Seebauer, R. Rutkowski, M. Schuster, S. Bekeschus, and P. Metelmann, "Treating cancer with cold physical plasma: On the way to evidence-based medicine," *Contrib. Plasma Phys.*, vol. 58, no. 5, pp. 415–419, Jun. 2018, doi: 10.1002/ctpp.201700085.

[20] F. Brehmer *et al.*, "Alleviation of chronic venous leg ulcers with a hand-held dielectric barrier discharge plasma generator (PlasmaDerm((R)) VU-2010): Results of a monocentric, two-armed, open, prospective, randomized and controlled trial (NCT01415622)," *J. Eur. Acad. Dermatol. Venereol.*, vol. 29, no. 1, pp. 148–55, Jan. 2015, doi: 10.1111/jdv.12490.

[21] S. Emmert *et al.*, "Atmospheric pressure plasma in dermatology: Ulcus treatment and much more," *Clin. Plasma Med.*, vol. 1, no. 1, pp. 24–29, 2013, doi: 10.1016/j.cpme.2012.11.002.

[22] C. Ulrich *et al.*, "Clinical use of cold atmospheric pressure argon plasma in chronic leg ulcers: A pilot study," *J. Wound Care*, vol. 24, no. 5, pp. 198–200, May 2015, doi: 10.12968/jowc.2015.24.5.196.

[23] A. Privat-Maldonado *et al.*, "ROS from physical plasmas: Redox chemistry for biomedical therapy," *Oxidative Med. Cellular Longevity*, vol. 2019, Oct. 2019, Art. no. 9062098, doi: 10.1155/2019/9062098.

[24] A. Schmidt, S. Bekeschus, K. Wende, B. Vollmar, and T. von Woedtke, "A cold plasma jet accelerates wound healing in a murine model of full-thickness skin wounds," *Exp. Dermatol.*, vol. 26, no. 2, pp. 156–162, Feb. 2017, doi: 10.1111/exd.13156.

[25] D. Shome, T. von Woedtke, K. Riedel, and K. Masur, "The HIPPO transducer YAP and its targets CTGF and Cyr61 drive a paracrine signalling in cold atmospheric plasma-mediated wound healing," *Oxidative Med. Cellular Longevity*, vol. 2020, pp. 1–14, Feb. 2020, doi: 10.1155/2020/4910280.

[26] A. Schmidt and S. Bekeschus, "Redox for repair: Cold physical plasmas and Nrf_2 signaling promoting wound healing," *Antioxidants*, vol. 7, no. 10, p. 146, Oct. 2018, doi: 10.3390/antiox7100146.

[27] A. Schmidt, T. von Woedtke, B. Vollmar, S. Hasse, and S. Bekeschus, "Nrf_2 signaling and inflammation are key events in physical plasma-spurred wound healing," *Theranostics*, vol. 9, no. 4, pp. 1066–1084, 2019, doi: 10.7150/thno.29754.

[28] M. Jayachandran, S. Rodriguez, E. Solis, J. Lei, and A. Godavarty, "Critical review of noninvasive optical technologies for wound imaging," *Adv. Wound Care*, vol. 5, no. 8, pp. 349–359, Aug. 2016, doi: 10.1089/wound.2015.0678.

[29] G. Lu and B. Fei, "Medical hyperspectral imaging: A review," *J. Biomed. Opt.*, vol. 19, no. 1, Jan. 2014, Art. no. 10901, doi: 10.1117/1.JBO.19.1.010901.

[30] G. Daeschlein *et al.*, "Hyperspectral imaging as a novel diagnostic tool in microcirculation of wounds," *Clin. Hemorheol. Microcirculation*, vol. 67, nos. 3–4, pp. 467–474, 2017.

[31] E. Grambow *et al.*, "Hyperspectral imaging for monitoring of perfusion failure upon microvascular anastomosis in the rat hind limb," *Microvascular Res.*, vol. 116, pp. 64–70, Mar. 2018, doi: 10.1016/j.mvr.2017.10.005.

[32] L. Khaodhiar *et al.*, "The use of medical hyperspectral technology to evaluate microcirculatory changes in diabetic foot ulcers and to predict clinical outcomes," *Diabetes Care*, vol. 30, no. 4, pp. 903–10, Apr. 2007, doi: 10.2337/dc06-2209.

[33] G. Daeschlein *et al.*, "Hyperspectral imaging: Innovative diagnostics to visualize hemodynamic effects of cold plasma in wound therapy," *Biomed. Technol.*, vol. 63, no. 65, pp. 603–608, May 2018, doi: 10.1515/bmt-2017-0085.

[34] D. L. Farkas and D. Becker, "Applications of spectral imaging: Detection and analysis of human melanoma and its precursors," *Pigment Cell Res.*, vol. 14, no. 1, pp. 2–8, Feb. 2001, doi: 10.1034/j.1600-0749.2001.140102.x.

[35] M. Wahabzada *et al.*, "Monitoring wound healing in a 3D wound model by hyperspectral imaging and efficient clustering," *PLoS ONE*, vol. 12, no. 12, 2017, Art. no. e0186425, doi: 10.1371/journal.pone.0186425.

[36] D. Myers, M. McGraw, M. George, K. Mulier, and G. Beilman, "Tissue hemoglobin index: A non-invasive optical measure of total tissue hemoglobin," *Crit Care*, vol. 13, no. S5, p. S2, 2009, doi: 10.1186/cc8000.

[37] A. Holmer *et al.*, "Oxygenation and perfusion monitoring with a hyperspectral camera system for chemical based tissue analysis of skin and organs," *Physiol. Meas.*, vol. 37, no. 11, pp. 2064–2078, Nov. 2016, doi: 10.1088/0967-3334/37/11/2064.

[38] A. Kulcke, A. Holmer, P. Wahl, F. Siemers, T. Wild, and G. Daeschlein, "A compact hyperspectral camera for measurement of perfusion parameters in medicine," *Biomed. Technol.*, vol. 63, no. 5, pp. 519–527, 2018, doi: 10.1515/bmt-2017-0145.

[39] F. Tetschke *et al.*, "Hyperspectral imaging for monitoring oxygen saturation levels during normothermic kidney perfusion," *J. Sensors Sensor Syst.*, vol. 5, no. 2, pp. 313–318, 2016, doi: 10.5194/jsss-5-313-2016.

[40] G. C. Baranowski and T. F. Chen, "Optical properties of skin surface," *Agache's Measuring the Skin*. Cham, Switzerland: Springer, 2017, doi: 10.1007/978-3-319-32383-1_9.

[41] S. Arndt, P. Unger, M. Berneburg, A. K. Bosserhoff, and S. Karrer, "Cold atmospheric plasma (CAP) activates angiogenesis-related molecules in skin keratinocytes, fibroblasts and endothelial cells and improves wound angiogenesis in an autocrine and paracrine mode," *J. Dermatol. Sci.*, vol. 89, no. 2, pp. 181–190, Feb. 2018, doi: 10.1016/j.jdermsci.2017.11.008.

[42] M. Chatraie, G. Torkaman, M. Khani, H. Salehi, and B. Shokri, "*In vivo* study of non-invasive effects of non-thermal plasma in pressure ulcer treatment," *Sci. Rep.*, vol. 8, no. 1, p. 5621, Apr. 2018, doi: 10.1038/s41598-018-24049-z.

[43] C. Duchesne, S. Banzet, J. J. Lataillade, A. Rousseau, and N. Frescaline, "Cold atmospheric plasma modulates endothelial nitric oxide synthase signalling and enhances burn wound neovascularisation," *J. Pathol.*, vol. 249, no. 3, pp. 368–380, Nov. 2019, doi: 10.1002/path.5323.

[44] J. Ditzel and E. Standl, "The problem of tissue oxygenation in diabetes mellitus," *Acta Medica Scandinavica*, vol. 197, no. S578, pp. 49–58, 2009, doi: 10.1111/j.0954-6820.1975.tb06502.x.

[45] V. Hahn *et al.*, "Plasma-mediated inactivation of E. Coli: Influence of protein on wet surface and in liquid medium," *Plasma Process. Polym.*, vol. 16, no. 5, 2019, Art. no. 1800164, doi: 10.1002/ppap.201800164.

[46] R. Noubade *et al.*, "NRROS negatively regulates reactive oxygen species during host defence and autoimmunity," *Nature*, vol. 509, no. 7499, pp. 235–239, May 2014, doi: 10.1038/nature13152.

[47] S. Roy, S. Khanna, K. Nallu, T. K. Hunt, and C. K. Sen, "Dermal wound healing is subject to redox control," *Mol. Therapy*, vol. 13, no. 1, pp. 211–20, Jan. 2006, doi: 10.1016/j.ymthe.2005.07.684.

[48] J. L. Arbiser *et al.*, "Reactive oxygen generated by Nox_1 triggers the angiogenic switch," *Proc. Nat. Acad. Sci. USA*, vol. 99, no. 2, pp. 715–20, Jan. 2002, doi: 10.1073/pnas.022630199.

[49] S. Reuter *et al.*, "The influence of feed gas humidity versus ambient humidity on atmospheric pressure plasma jet-effluent chemistry and skin cell viability," *IEEE Trans. Plasma Sci.*, vol. 43, no. 9, pp. 3185–3192, Sep. 2015.

[50] A. Schmidt, S. Bekeschus, H. Jablonowski, A. Barton, K. D. Weltmann, and K. Wende, "Role of ambient gas composition on cold physical plasma-elicited cell signaling in keratinocytes," *Biophys. J.*, vol. 112, no. 11, pp. 2397–2407, Jun. 2017, doi: 10.1016/j.bpj.2017.04.030.

[51] J. Li, Y. P. Zhang, and R. S. Kirsner, "Angiogenesis in wound repair: Angiogenic growth factors and the extracellular matrix," *Microscopy Res. Techn.*, vol. 60, no. 1, pp. 107–14, Jan. 2003, doi: 10.1002/jemt.10249.

[52] A. Barton *et al.*, "Nonthermal plasma increases expression of wound healing related genes in a keratinocyte cell line," *Plasma Med.*, vol. 3, no. 1–2, pp. 125–136, 2013, doi: 10.1615/PlasmaMed.2014008540.

[53] A. Schmidt, S. Bekeschus, K. Jarick, S. Hasse, T. von Woedtke, and K. Wende, "Cold physical plasma modulates p53 and mitogen-activated protein kinase signaling in keratinocytes," *Oxidative Med. Cellular Longevity*, vol. 2019, pp. 1–16, Jan. 2019, doi: 10.1155/2019/7017363.

[54] A. Schmidt *et al.*, "One year follow-up risk assessment in SKH-1 mice and wounds treated with an argon plasma jet," *Int. J. Mol. Sci.*, vol. 18, no. 4, pp. 1–16, Apr. 2017, doi: 10.3390/ijms18040868.

[55] J. Scallan, V. H. Huxley, and R. J. Korthuis, "Capillary fluid exchange: Regulation, functions, and pathology," *Colloquium Series Integr. Syst. Physiol. Mol. Function*, vol. 2, no. 1, pp. 1–94, 2010.

[56] T. Borchardt *et al.*, "Effect of direct cold atmospheric plasma (diCAP) on microcirculation of intact skin in a controlled mechanical environment," *Microcirculation*, vol. 24, no. 8, Nov. 2017, Art. no. e12399, doi: 10.1111/micc.12399.

[57] R. Rutkowski *et al.*, "Hyperspectral imaging for *in vivo* monitoring of cold atmospheric plasma effects on microcirculation in treatment of head and neck cancer and wound healing," *Clin. Plasma Med.*, vols. 7–8, pp. 52–57, Dec. 2017, doi: 10.1016/j.cpme.2017.09.002.

[58] S. Hyttel-Sorensen, T. W. Hessel, and G. Greisen, "Peripheral tissue oximetry: Comparing three commercial near-infrared spectroscopy oximeters on the forearm," *J. Clin. Monitor Comput.*, vol. 28, no. 2, pp. 149–55, Apr. 2014, doi: 10.1007/s10877-013-9507-9.

[59] A. Holmer, J. Marotz, P. Wahl, M. Dau, and P. W. Kämmerer, "Hyperspectral imaging in perfusion and wound diagnostics–methods and algorithms for the determination of tissue parameters," *Biomedizinische Technik*, vol. 63, no. 5, pp. 547–556, 2018.